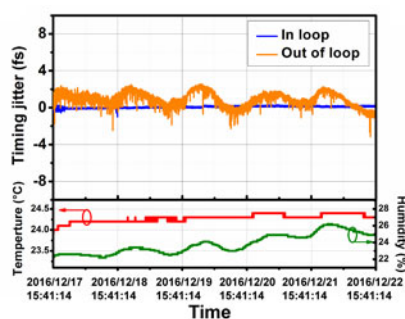# Optical–Optical Synchronization Between Two Independent Femtosecond Yb-Fiber Lasers With 10^{-20} Instability in 10^5 s

Haochen Tian
Youjian Song
Jiahe Yu
Haosen Shi
Minglie Hu

(a)

(b)

IEEE
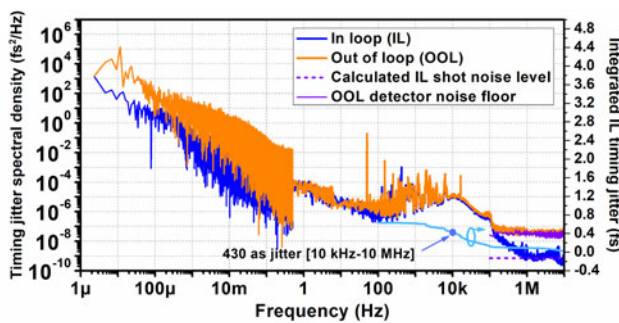
Optical–Optical Synchronization Between Two Independent Femtosecond Yb-Fiber Lasers With 10^{-20} Instability in 10^5 s

Haochen Tian [ID], Youjian Song [ID], Jiahe Yu, Haosen Shi, and Minglie Hu [ID]

Ultrafast Laser Laboratory, Key Laboratory of Opto-Electronic Information Technology, Ministry of Education, School of Precision Instrument and Opto-Electronics Engineering, Tianjin University, Tianjin 300072, China

Abstract: Optical–optical synchronization between independent mode-locked lasers with attosecond timing precision is essential for arbitrary electric-field waveform generation, sub-cycle optical pulse synthesis, optical frequency transfer as well as next-generation photon-science facilities, e.g., X-ray free-electron lasers. Long-term stable operation with low timing drift is highly desired for all above applications. Here, we present a five-day uninterrupted timing synchronization between two independent femtosecond Yb-fiber lasers via balanced optical correlation method. The out-of-loop residual timing drift over the entire time frame reaches 733 as rms, corresponding to 1.36×10^{-20} instability at 1.31×10^5 s. To the best of our knowledge, it is the first characterization of 10^5 s instability for subfemtosecond optical–optical synchronization based on mode-locked lasers.

Index Terms: Timing synchronization, mode-locked lasers, timing jitter, balanced optical cross-correlation, attosecond photonics.

1. Introduction

Passively mode-locked lasers inherently emit well-defined ultrashort pulse trains with sub-femtosecond timing jitter, providing an extremely precise timing reference by phase-locking to a rf/optical atomic clock [1]–[3]. Tight synchronization among mode-locked lasers, which is so-called optical-optical synchronization, allows a femtosecond precision timing network [4], which is indispensable for advanced pump-probe experiments that resolve sub-atomic dynamics based on large scale scientific facilities, such as particle accelerators and X-ray free-electron lasers (XFELs) [5], [6]. Furthermore, optical-optical synchronization has been applied to phase-lock optical frequency combs at different sites, making possible simultaneous transfer of radio and optical time/frequency standards through a fiber [7] or free space link [8], [9]. Timing synchronization among local femtosecond lasers is also very important because it is an essential prerequisite towards coherent optical pulse synthesis [10]–[12], which enables sub-cycle optical pulses synthesis as well as arbitrary optical electric-field waveform generation.

There has been rapid progress on the timing synchronization between independent mode-locked lasers owing to the recent advances in ultrafast laser stabilization techniques. Passive, active as

well as hybrid schemes towards optical-optical synchronization have been demonstrated. In 2001, Z. Wei *et al.* reported a passive synchronization technique between Ti:Sapphire femtosecond laser and Cr:forsterite femtosecond laser by crossing of both laser pulses in a Kerr medium. The typical timing jitter derived from the cross correlation is less than 3 fs [13]. Passive synchronization can also be achieved by using master-slave injecting locking method [14] or by sharing a common saturable absorber [15]. Active synchronization based on optical cross correlation proves to be the most reliable approach enabling both ultralow residual jitter and long term stability [16]–[21]. In 2003, T. R. Schibli *et al.* firstly achieved attosecond active synchronization of passively mode-locked lasers by means of balanced optical cross correlation (BOC) [17]. With the same approach, H. Li *et al.* remotely synchronized the repetition rate of a Ti:sapphire laser and a Er-doped fiber laser through a 360 m length-stabilized fiber link. The drift between two optical oscillators is 3.3 fs rms over 24 hours [19]. In 2017, M. Xin *et al.* presented a remote optical-optical synchronization across 3.5-km fiber link. The rms timing jitter over 44 hours is below 100 as owing to implementing a novel polarization-noise-suppressed BOC (PNS-BOC) [20], [21]. Besides the above, a hybrid synchronization approach [22]–[24] has also been frequently used, which significantly releases the critical phase-locked loop design because the high bandwidth active synchronization can be avoided.

Active optical-optical synchronization between independent mode-locked lasers is very sensitive to mode-locking instability and environmental disturbance. Slight pump fluctuation or transient acoustic event easily breaks the phase-locked loop, particularly when extremely high precision synchronization is established. Nevertheless, robust operation with long term stability is essential for a practical optical-optical synchronization. For instance, long term non-interrupted date acquisition is routinely required for XFEL-based time-resolved pump-probe experiments so as to record a complete molecular movie [25]. Not that Yb-fiber laser sources, due to the exceptional average power scalability, has been playing an increasingly important role in such XFEL systems [26]. In this letter, we characterize, for the first time, the long term instability of optical-optical synchronization in 10^5 s averaging time. Two home-built mode-locked Yb-fiber lasers operating at stretched pulse regime are optically synchronized by means of BOC method. Tight optical-optical synchronization sustained for 5 days (120 hours), which is $\sim$3 times longer than the existing performance [20], [21]. An optical cross-correlator has been used for independent out-of-loop (OOL) timing error detection. The out-of-loop residual timing drift is as low as 733 as rms and the timing instability evaluated by the overlapping Allan deviation reaches 1.36×10^{-20} at 1.31×10^5 s. The performance can be further improved by using a precisely temperature controlled OOL optical cross-correlator.

2. Experimental Setup and Results

The experimental setup is shown in Fig. 1. Two nearly identically built nonlinear polarization evolution (NPE) mode-locked Yb-fiber lasers with repetition rates of 157 MHz are implemented for long-term optical-optical timing synchronization. With carefully optimization of intracavity grating separations, the lasers work in a stretched pulse mode-locking regime with close to zero cavity dispersion so as to avoid Gordon-Haus jitter [2]. The exact cavity dispersion is slightly negative for the sake of achieving ultralow quantum-limited timing jitter and ultra-stable mode-locking at the same time [27]. Here, sub-femtosecond quantum-limited timing jitter is a prerequisite for high precision timing synchronization, while stable mode-locking is crucial for long term operation of optical-optical synchronization. The output average power (pulse energy) of the two lasers is 85 mW (0.54 nJ) and 65 mW (0.43 nJ). Two outputs are extracavity dechirped by a Gires–Tournois Interferometer mirror pairs, obtaining pulse durations of 77 and 69 fs, respectively.

The dechirped output from each laser is combined at a polarization beam splitter (PBS). Nearly half the output power is directed to balanced cross correlator for timing synchronization. To achieve balanced cross correlation, two pulse trains with orthogonal polarization states are focused into a 0.65-mm thick, type-II phase matched beta-barium borate (BBO) crystal for sum frequency generation (SFG). The SFG signals are detected by a high-speed balanced photodetector (BPD, Newfocus,
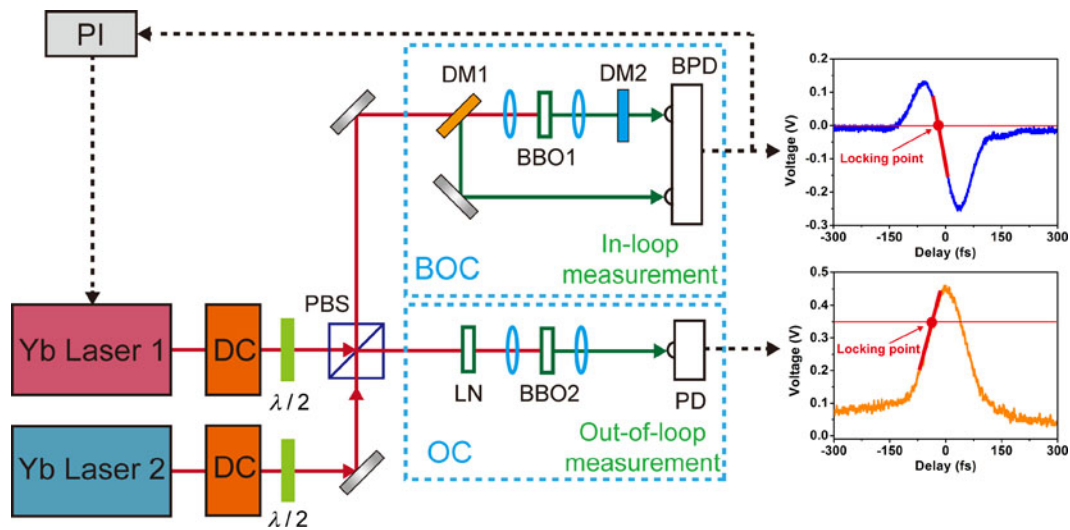
Fig. 1. Experimental setup. BBO, beta-barium borate; BPD, Balanced photodetector; BOC, balanced optical cross-correlator; DC, dispersion compensation; DM, dichroic mirror; DM1, AR at 1040 nm, HR at 520 nm; DM2, AR at 520 nm, HR at 1040 nm; OC, optical cross-correlator; LN, lithium niobate; PBS, polarization beam spliter; PD, photodetector; PI, proportional-integral servo (Newfocus, LB1005).

Model 1807) with a cutoff frequency of ∼80 MHz. The SFG process effectively converts the relative timing jitter between pulse trains to a proportionate intensity fluctuation. In order to eliminate the contribution that originates from inherent intensity noise of the two pulse trains, the pulse trains after transmission from BBO are reflected back by a dichroic mirror (DM2) for another identical SFG. Meanwhile, the birefringence of BBO crystal produces additional ∼100 fs temporal delay between two cross correlations. After that, subtraction in the BPD leads to an S-shaped timing discrimination curve, as shown in the inset of Fig. 1. The linear range, as indicated by a red line in the curve, characterizes an in-loop (IL) timing error discrimination slope of 6.0 mV/fs. The error voltage is feedback upon one intracavity piezo-actuated mirror inside one Yb-fiber laser and, thus, closes the phase-locked loop for timing synchronization. Fast-response actuator is important to establish the phase-locking and to maintain it for a long time. Here, a ceramic piezo actuator (PI, PL055.31) with 2.2 μm maximum displacement is implemented. The piezo-actuated mirror is mounted upon a high precision stepper motor, which helps to compensate for long term drifts considering the limited displacement range of the piezo actuator.

An independent single-pass optical cross-correlator is used for OOL residual timing jitter measurement, as shown in Fig. 1. The single-pass cross-correlation is based on SFG in a piece of 1 mm-thick type-II phase-matched BBO. A 0.4-mm thick lithium niobate (LN) provides extra bire-fringence between two pulse trains, ensuring that an appropriate pulse timing overlapping. The cross-correlation trace before timing synchronization has been characterized, as shown in the inset of Fig. 1. The cross correlator outputs at a mean voltage of ∼ 350 mV after the establishment of op-tical phase-locking, indicating that the cross correlator works at its linear range, i.e., the two pulses are offset in time by ∼1/2 the pulse width. The timing error discrimination slope reads ∼4.0 mV/fs. Comparing to interferometer-based OOL scheme with a variable delay line as in [28], this common path OOL configuration setup is immune from additive timing drifts originated from mechanical vibration induced differential optical path fluctuations.

The entire setup is built upon a vibration-isolated optical table. Particularly, an aluminum cover with foams glued on the inner side is used to shield the two Yb-fiber lasers. Lead foam is placed underneath the breadboard so as to further dampen table vibrations. By doing so, acous-tic noise can be well isolated from the setup, enabling long term timing synchronization. Air-conditioner works continuously during the experiment. The room temperature is maintained at 24.1 ± 0.3 °C.
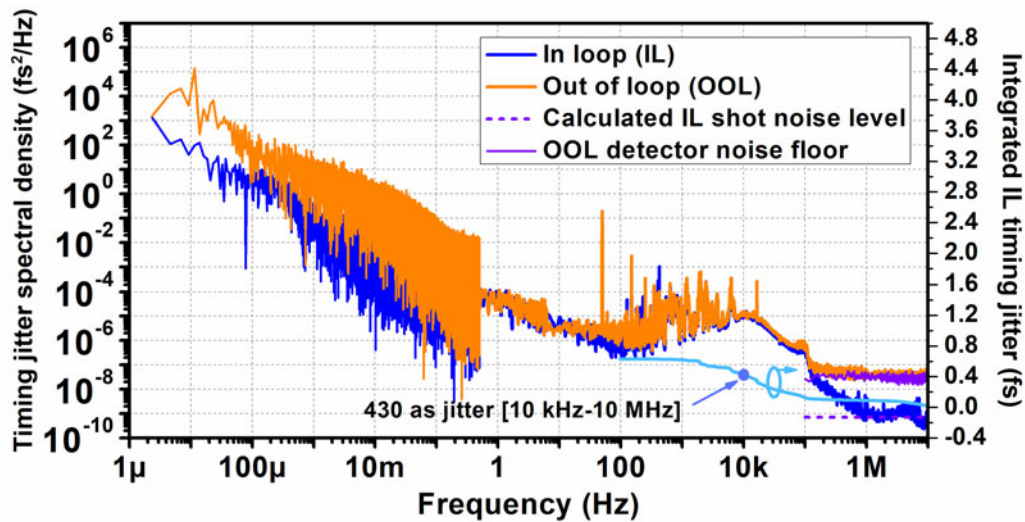
Fig. 2. The residual IL (blue line), OOL (orange line) timing jitter power spectral density and integrated IL timing jitter (light blue line) after timing synchronization. The OOL detector noise floor (magenta line) and the calculated IL shot noise level (magenta dashed line) are also shown in the same figure.

After tight repetition rate locking is achieved, both the IL and OOL jitter spectral density are characterized, as shown in Fig. 2. The lower frequency (0.5 Hz to 100 kHz) and higher frequency (>100 kHz) spectra are obtained by FFT analyzer (Standard Research, SR770) and RF spectral analyzer (Agilent, 8560EC), respectively. The jitter power spectral density (PSD) reflects a locking bandwidth of ∼11 kHz. Beyond the locking bandwidth, the IL (OOL) jitter spectra basically follows a characteristic −20 dB/decade slope from 10 kHz to 1 MHz (from 10 kHz to 100 kHz), indicating a random walk nature of free running pulse train timing jitter directly induced by ASE noise in the gain fiber. The IL measurement above 1 MHz Fourier frequency is limited by detection shot noise, while the OOL measurement reaches detector thermal noise floor above 100 kHz Fourier frequency. The integrated timing jitter derived from the IL PSD is also shown in Fig. 2, revealing that the quantum limited timing jitter (sum of the two lasers) is 430 as rms, integrated from 10 kHz to 10 MHz.

Synchronization of two lasers operates uninterruptedly for 5 days (120 h). We sample the IL and OOL residual error signals at 1 kHz through a data acquisition board (National Instruments, NI USB-6008). In the meanwhile, the temperature and relative humidity in the laboratory are logged with 0.1 C and 0.1% resolution, respectively, as shown in Fig. 3(a). The IL (OOL) residual timing drifts between two synchronized lasers are 103 as rms (733 as rms). The PSDs of the IL (OLL) time series have also been derived and plotted in the lower Fourier frequency regime (from 2 μHz to 0.5 Hz) of Fig. 2. The 1/f characteristics at low Fourier frequency reveals a slow timing drift for both IL and OOL timing synchronization. Particularly, the OOL residual timing error oscillates with a period of ∼24 h (1 day) at amplitude of ∼1.5 fs, showing an evident environmental dependency. For a more in-depth investigation, a 24-hour controlled experiment without temperature stabilization has been conducted, as shown in Fig. 3(b). The experimental result indicates that temperature stabilization is highly desired to retard OLL timing drift, otherwise, the OOL timing synchronization degrades rapidly.

The frequency instability of the optical-optical synchronization has been evaluated by Allan deviation and time deviation. The overlapping Allan deviation is the most common measurement of time-domain frequency stability. It is a most widely used form of the normal Allan deviation, which makes maximum use of a data set by forming all possible overlapping samples at each averaging time. Fig. 4(a) shows the overlapping Allan deviation calculated from IL and OOL residual timing error, respectively. The overlapping Allan deviation for residual IL timing error characterizes a
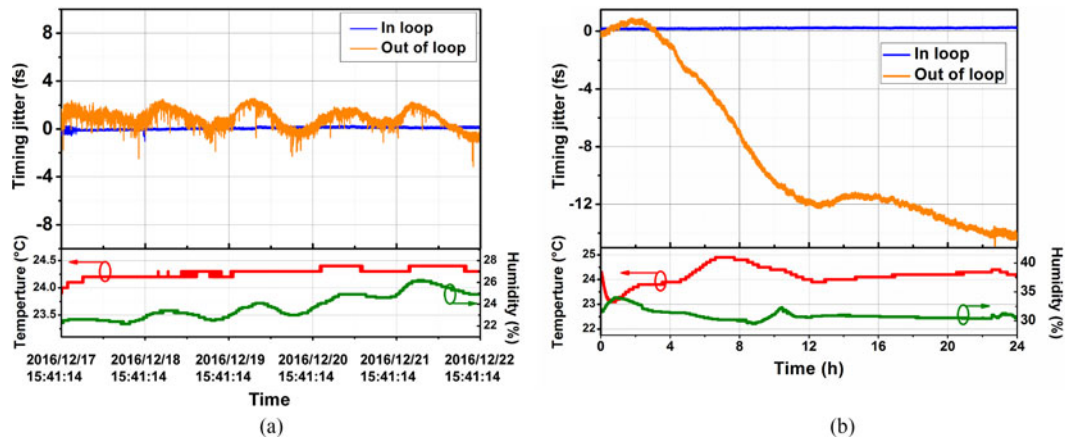
Fig. 3. (a) Long term residual IL (blue curve) and OOL (orange curve) timing drifts. Temperature (red curve) and relative humidity (green curve) in the laboratory are also shown. (b) 24 hours synchronization results without environmental temperature stabilization.
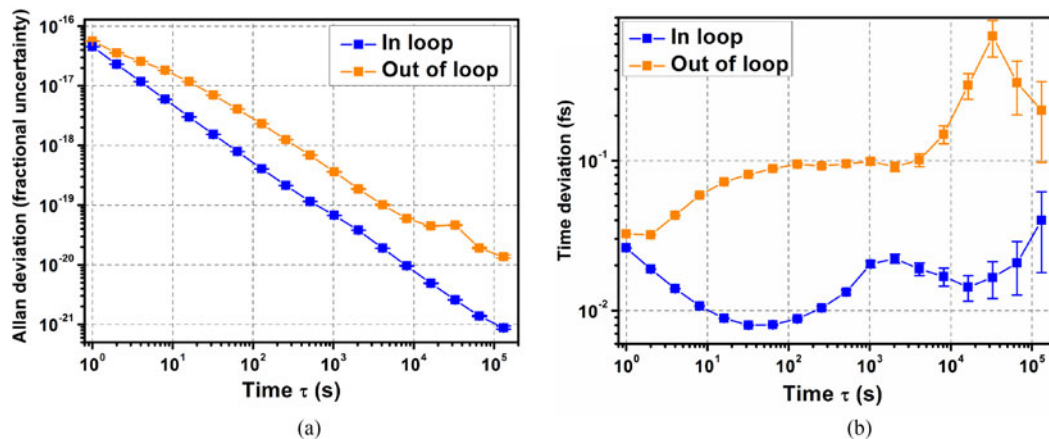

Fig. 4. Timing instability of long term synchronization. (a) IL (blue solid square) and OOL (orange solid square) overlapping Allan deviation; (b) IL (blue solid square) and OOL (orange solid square) timing Allan deviation.

$1/\tau$-slope and falls to 8.76×10^{-22} at 1.31×10^5 s, whereas the overlapping Allan deviation for OOL timing error is about 10 dB higher due to the temperature-change induced cyclic timing drift. The OOL timing instability reaches 1.36×10^{-20} at 1.31×10^5 s.

The time deviation (TDEV) [29] is a measure of time stability based on the modified Allan variance. It is particularly useful for measuring the stability of a time distribution network. The IL and OOL TDEVs are shown in Fig. 4(b). The IL timing deviation averages down as $\sqrt{\tau}$ until 32 s and then reaches a floor, which indicates a $\sim 1/f$ increase in the jitter PSD for f< 0.03 Hz. On the other hand, the OOL timing deviation reflects a non-white jitter PSD for f< 1Hz. As already discussed above, we attribute the non-white OOL timing fluctuation at low Fourier frequencies to drift of OOL optical cross correlator induced by environmental changes. Note that, laser intensity noise may also add to the OOL timing noise since OC is used for timing error characterization instead of BOC. However, as shown from Fig. 2, the OOL PSD derived from OC overlaps very well with the IL trace at lower Fourier frequency (<100 kHz). This means that the contribution of laser intensity noise is negligible during OOL synchronization performance evaluation.

3. Conclusion

In this paper, we demonstrate an uninterrupted sub-femtosecond precision optical-optical synchronization between independent Yb-fiber lasers for 5 days (120 hours) by means of BOC method. The long term stable tight synchronization is attributed to quantum-limited timing jitter optimization as well as mode-locking stability improvement via cavity dispersion management. Meanwhile, the implementation of a >10 kHz phase-locked loop which compensates for random repetition rate changes induced by high frequency acoustic noise is crucial to maintain long term phase-locking. As a result, the OOL residual timing drift is as low as 733 as rms and the timing instability evaluated by the overlapping Allan deviation reaches 1.36×10^{-20} at 1.31×10^5 s. For the first time, the long term instability of optical-optical synchronization between mode-locked lasers is evaluated at $\sim 10^5$ s averaging time. This result is a key step towards the real-world applications of the emerging sub-cycle optical pulse synthesis, optical frequency standard transfer and XFEL-based time-resolved sciences.

Acknowledgment

References

[1] A. J. Benedick, J. G. Fujimoto, and F. X. Kärtner, "Optical flywheels with attosecond jitter," *Nature Photon.*, vol. 6, no. 2, pp. 97–100, 2012.

[2] J. Kim and Y. Song, "Ultralow-noise mode-locked fiber lasers and frequency combs: Principles, status, and applications," *Adv. Opt. Photon.*, vol. 8, no. 3, pp. 465–540, 2016.

[3] J. Kim, K. Jung, J. Shin, C. G. Jeon, and D. Kwon, "Femtosecond laser-based microwave signal generation and distribution," *J. Lightw. Technol.*, vol. 34, no. 20, pp. 4631–4638, Oct. 2016.

[4] J. Kim, J. A. Cox, J. Chen, and F. X. Kärtner, "Drift-free femtosecond timing synchronization of remote optical and microwave sources," *Nature Photon.*, vol. 2, no. 12, pp. 733–736, 2008.

[5] J. Ullrich, A. Rudenko, and R. Moshammer, "Free-electron lasers: New avenues in molecular physics and photochemistry," *Annu. Rev. Phys. Chem.*, vol. 63, no. 1, pp. 635–660, 2012.

[6] S. Schulz *et al.*, "Femtosecond all-optical synchronization of an X-ray free-electron laser," *Nature Commun.*, vol. 6, 2015, Art. no. 5938.

[7] X. Chen *et al.*, "Simultaneously precise frequency transfer and time synchronization using feed-forward compensation technique via 120 km fiber link," *Sci. Rep.*, vol. 5, 2015, Art. no. 18343.

[8] F. R. Giorgetta, W. C. Swann, L. C. Sinclair, E. Baumann, I. Coddington, and N. R. Newbury, "Optical two-way time and frequency transfer over free space," *Nature Photon.*, vol. 7, no. 6, pp. 434–438, 2013.

[9] J. D. Deschênes *et al.*, "Synchronization of distant optical clocks at the femtosecond level," *Phys. Rev. X*, vol. 16, no. 1, pp. 519–530, 2016.

[10] R. K. Shelton, L. S. Ma, H. C. Kapteyn, M. M. Murnane, J. L. Hall, and J. Ye, "Phase-coherent optical pulse synthesis from separate femtosecond lasers," *Science*, vol. 293, no. 5533, pp. 1286–1289, 2001.

[11] J. A. Cox, W. P. Putnam, A. Sell, A. Leitenstorfer, and F. X. Kärtner, "Pulse synthesis in the single-cycle regime from independent mode-locked lasers using attosecond-precision feedback," *Opt. Lett.*, vol. 37, no. 17, pp. 3579–3581, 2012.

[12] H. Tian, Y. Song, F. Meng, Z. Fang, M. Hu, and C. Wang, "Long-term stable coherent beam combination of independent femtosecond Yb-fiber lasers," *Opt. Lett.*, vol. 41, no. 22, pp. 5142–5145, 2016.

[13] Z. Wei, Y. Kobayashi, Z. Zhang, and K. Torizuka, "Generation of two-color femtosecond pulses by self-synchronizing Ti:sapphire and Cr:forsterite lasers," *Opt. Lett.*, vol. 26, no. 22, pp. 1806–1808, 2001.

[14] D. Yoshitomi and K. Torizuka, "Long-term stable passive synchronization between two-color mode-locked lasers with the aid of temperature stabilization," *Opt. Exp.*, vol. 22, no. 4, pp. 4091–4097, 2014.

[15] M. Zhang, E. J. R. Kelleher, A. S. Pozharov, E. D. Obraztsova, S. V. Popov, and J. R. Taylor, "Passive synchronization of all-fiber lasers through a common saturable absorber," *Opt. Lett.*, vol. 36, no. 20, pp. 3984–3986, 2011.

[16] L. S. Ma, R. K. Shelton, H. C. Kapteyn, M. M. Murnane, and J. Ye, "Sub-10-femtosecond active synchronization of two passively mode-locked Ti:sapphire oscillators," *Phys. Rev. A*, vol. 64, no. 2, pp. 130–131, 2001.

[17] T. R. Schibli *et al.*, "Attosecond active synchronization of passively mode-locked lasers by balanced cross correlation," *Opt. Lett.*, vol. 28, no. 11, pp. 947–949, 2003.

[18] T. Minamikawa, N. Tanimoto, M. Hashimoto, and T. Araki, "Jitter reduction of two synchronized picosecond mode-locked lasers using balanced cross-correlator with two-photon detectors," *Appl. Phys. Lett.*, vol. 89, 2006, Art. no. 191101.

[19] H. Li *et al.*, "Remote two-color optical-to-optical synchronization between two passively mode-locked lasers," *Opt. Lett.*, vol. 39, no. 18, pp. 5325–5328, 2014.

[20] M. Xin *et al.*, "Attosecond precision multi-kilometer laser-microwave network," *Light, Sci. Appl.*, vol. 6, 2017, Art. no. e16187.

[21] M. Xin *et al.*, "Breaking the femtosecond barrier in multi-kilometer timing synchronization systems," *IEEE J. Sel. Topics Quantum Electron.*, vol. 23, no. 3, 2017, Art. no. 8800212.

[22] D. Yoshitomi, Y. Kobayashi, H. Takada, M. Kakehata, and K. Torizuka, "100-attosecond timing jitter between two-color mode-locked lasers by active–passive hybrid synchronization," *Opt. Lett.*, vol. 30, no. 11, pp. 1408–1410, 2005.

[23] B.-W. Tsai, S.-Y. Wu, C. Hu, W.-W. Hsiang, and Y. Lai, "Subfemtosecond hybrid synchronization between ultrafast Yb and Er fiber laser systems by controlling the relative injection timing," *Opt. Lett.*, vol. 38, no. 17, pp. 3456–3459, 2013.

[24] B.-J. Fong, W.-T. Lin, S.-Y. Wu, J.-L. Peng, W.-W. Hsiang, and Y. Lai, "Relative carrier-envelope phase stabilization of hybridly synchronized ultrafast Yb and Er fiber-laser systems with the feed-forward scheme," *Opt. Lett.*, vol. 40, no. 6, pp. 966–969, 2015.

[25] J. M. Glownia *et al.*, "Time-resolved pump-probe experiments at the LCLS," *Opt. Exp.*, vol. 18, no. 17, pp. 17620–17630, 2010.

[26] M. J. Prandolini, R. Eiedel, M. Schulz, and F. Tavella, "A review of high power OPCPA technology for high repetition rate free-electron lasers," in *Proc. 2014 Free Electron Laser Conf.*, 2014, Paper TUA02.

[27] Y. Song, C. Kim, K. Jung, H. Kim, and J. Kim, "Timing jitter optimization of mode-locked Yb-fiber lasers toward the attosecond regime," *Opt. Exp.*, vol. 19, no. 15, pp. 14518–14525, 2011.

[28] P. Qin *et al.*, "Reduction of timing jitter and intensity noise in normal-dispersion passively mode-locked fiber lasers by narrow band-pass filtering," *Opt. Exp.*, vol. 22, no. 23, pp. 28276–28283, 2014.

[29] W. J. Riley, *Handbook of Frequency Stability Analysis*. Gaithersburg. MD, USA: *NIST Special Publication 1065*, 2008.